

Model Based Fault Detection of Wind Turbine Drive Trains

Marc Hilbert*, Christiane Küch, Karl Nienhaus

Institute for Mining and Metallurgical Machinery, RWTH Aachen University, Aachen, Germany
mhilbert@imr.rwth-aachen.de

Wind turbines are fundamental components of power conversion. With the increasing number of wind turbines worldwide, the exposure to harsh environmental conditions and the use of remote areas like offshore, arctic or desert regions, it has become important to predict abnormal machine behaviour as early as possible. Therefore, automated fault detection is necessary. Fault detection will prevent extensive damage in case of a fault and create time to react to faults, for example, to prepare inspections and/or to purchase spare parts. To reduce the downtime of wind turbines, fault detection systems are already widely used but more research and development need to be done. The diagnostic approach of those systems is to use pre-set fixed alert thresholds but has several drawbacks and therefore makes fault isolation difficult. To overcome the drawbacks of the common systems, this paper introduces model based condition monitoring using residual generation to wind turbine drive trains. Residuals describe the difference between the measurements and the model output. The model output represents the non-faulty system behaviour. If the measurement deviates from the model output a fault is indicated. Residual generation is a known approach for other systems. A mathematical model of a system, such as a wind turbine drive train, depends on the actual and past machine operation as well as on the ambient conditions. By knowing these conditions and being able to describe them in an analytic way, a model can be derived using the well-known state-space representation.

1. Introduction

The task of fault detection is to detect faults as early as possible. Gertler (1988) divides fault detection in two major groups: model based methods and non-model based methods. Some examples of non-model based fault detection are (adapted from Gertler, 1988): pre-set alert thresholds, multiple sensors and frequency analysis. Especially the method of pre-set alert thresholds is widely used in fault detection because of its simplicity, but this method also has several drawbacks (adapted from Gertler, 1991): thresholds need to be set conservatively because of a possibly wide range of signal variation. Another drawback is that fault detection in transient stages because the non-faulty signal and the fault need to add up until the pre-set alert threshold is exceeded. To overcome these drawbacks, the model based approach was introduced with the following benefits: early detection of faults, monitoring signals also in transient operating states and fault detection in closed loop systems (Isermann, 1995).

This paper applies the model based fault detection on a wind turbine generator to detect temperature faults as early as possible. It is pointed out in Faulstich (2012) that the major faults of the generator cause a mean annual downtime of 5.7 days. Together with the electrical system (0.80 days of mean annual downtime), the electrical control (0.63) and the gearbox (0.59), the generator (0.58) is one of the top reasons of turbine downtime. The presented method has to be understood as an additional tool to protect the machine against high temperature since high temperature reduces the remaining useful lifetime and causes faults.

The paper is organized as follows: introduction of the model, simulation and discussion of faults.

2. System Model

The discrete time invariant state-space representation is used to model the system behaviour, see equation (1) and (2).

$$\mathbf{x}(k+1) = \mathbf{A} \mathbf{x}(k) + \mathbf{B} \mathbf{u}(k), \quad \mathbf{x}(0) = \mathbf{x}_0 \quad (1)$$

$$\mathbf{y}(k) = \mathbf{C} \mathbf{x}(k) + \mathbf{D} \mathbf{u}(k). \quad (2)$$

Where \mathbf{A} , \mathbf{B} , \mathbf{C} and \mathbf{D} are constant matrices. The output is represented by $\mathbf{y}(k)$, the inputs by $\mathbf{u}(k)$, the state variables by $\mathbf{x}(k)$ and the estimated variables are marked with a circumflex. To compensate modelling uncertainties, an observer is added. The observer is an output observer and can be described as follows:

$$\hat{\mathbf{x}}(k+1) = \mathbf{A} \hat{\mathbf{x}}(k) + \mathbf{B} \mathbf{u}(k) + \mathbf{L} (\mathbf{y}(k) - \mathbf{C} \hat{\mathbf{x}}(k) - \mathbf{D} \mathbf{u}(k)) \quad (3)$$

$$\hat{\mathbf{y}}(k) = \mathbf{C} \hat{\mathbf{x}}(k) + \mathbf{D} \mathbf{u}(k). \quad (4)$$

The observer gain \mathbf{L} needs to be selected such that the system is stable, but model uncertainties are compensated. The observer and the modelled process are displayed in Figure 1.

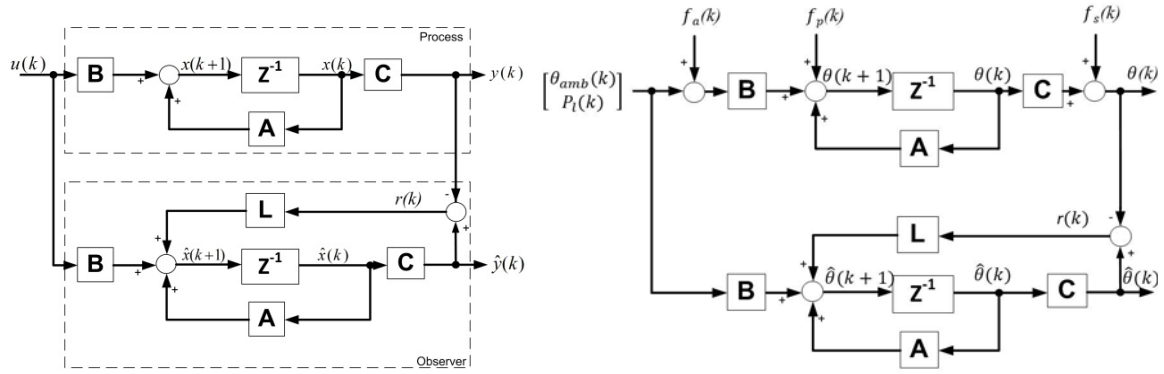


Figure 1: Block diagram of a generalized model and observer in state-space representation

Figure 2: Block diagram of the thermal model and the thermal observer in state-space representation including faults

3. Fault Diagnosis

To diagnose a faulty behaviour of the model based system, different methods are used to analyse the residual signal $\mathbf{r}(k)$ instead of the output signal $\mathbf{y}(k)$. The residual $\mathbf{r}(k)$ represents the difference between the measured signal $\mathbf{y}(k)$ and the observer output $\hat{\mathbf{y}}(k)$. Thereby, the observer output represents the ideal non-faulty system behaviour. In fact, the methods used to analyse $\mathbf{r}(k)$ are the same than the ones for $\mathbf{y}(k)$ but provide a more accurate fault diagnosis. (Ding, 2008) In this paper, we focus on the peak value \mathbf{J}_{peak} and the trend value \mathbf{J}_{trend} . Besides those two values methods, more can be found e.g. in Ding (2008).

3.1 Peak Value

Adapted from Ding (2008) the peak value \mathbf{J}_{peak} is defined as follows:

$$\mathbf{J}_{peak} = \|\mathbf{r}\|_{peak} := \sup_{k \geq 0} \|\mathbf{r}(k)\| \quad (5)$$

3.2 Trend Value

In Ding (2008) the trend value \mathbf{J}_{trend} is defined in equation (6). \mathbf{J}_{trend} provides information about the gradient between data points. For practical implementation, $\Delta \mathbf{r}(k)$ is replaced by $\Delta \mathbf{r}(k) = \mathbf{r}(k) - \mathbf{r}(k-1)$.

$$\mathbf{J}_{trend} = \|\Delta \mathbf{r}(k)\|_{peak} := \sup_{k \geq 0} \|\Delta \mathbf{r}(k)\| \quad (6)$$

3.3 Residual Threshold Monitoring

The introduced values J will be compared to a pre-set residual threshold J_{th} (the threshold for the peak value is $J_{th,peak}$ and the trend value $J_{th,trend}$) to test if a faulty behaviour is present. The monitoring can be formulated as

$J > J_{th} \Rightarrow$ a faulty behaviour is detected,

$J \leq J_{th} \Rightarrow$ no faulty behaviour is detected (Ding, 2008).

4. Fault Simulation

4.1 Model

To simulate the faulty behavior, a straightforward discrete thermal model of the wind turbine generator is designed in Nienhaus et al. (2012) and can be described in the following time invariant state-space representation with observer:

$$\hat{\theta}(k+1) = e^{-\frac{1}{RC}T} \hat{\theta}(k) + RC \left(1 - e^{-\frac{1}{RC}T}\right) \begin{bmatrix} \frac{1}{RC} & 1 \\ 1 & c \end{bmatrix} \begin{bmatrix} \theta_{amb}(k) \\ P_l(k) \end{bmatrix} - L \left(\hat{\theta}(k) - \theta(k)\right), \quad \hat{\theta}(0) = \theta(0) \quad (7)$$

$$\hat{\theta}(k) = \hat{\theta}(k) \quad (8)$$

Where $\theta(k)$ is the measured generator temperature (e.g. the stator winding temperature), $\hat{\theta}(k)$ is the estimated generator temperature, $P_l(k)$ are the power losses of the generator and $\theta_{amb}(k)$ the ambient temperature. The constant parameters thermal resistance R and thermal capacity C describe the thermal behavior of the generator. The sample time of the discrete model is T . The design as well as the parameter estimation is shown by the authors in Nienhaus et al. (2012). The corresponding block diagram is shown in Figure 2. In this paper, faults are applied to the thermal model as shown in Figure 2. With this approach, it can be tested if the fault detection is able to detect certain faults.

4.2 Fault Description

In this paper, we will design exclusively additive faults. The faults are denoted with f_a , f_p and f_s and shown in Figure 2. The faults are divided in three categories (Ding, 2008):

- sensor fault f_s : faults that affect the measurements directly,
- actuator fault f_a : faults that affect the actuator and
- process fault f_p : faults that are malfunctions of the process.

For the sensor fault, a bias of 15 K will be assumed, and the fault signal $f_s(k)$ will be generated with a step function as shown in Figure 3. To design an actuator fault, we assume a bias of 37.5 % of the value of the total power losses $P_l(k)$. The fault of $\theta_{amb}(k)$ is designed as a bias of 15 K. The faults will be simulated with step functions as shown in Figure 4 and Figure 5. The process fault is designed as a step function as shown in Figure 6.

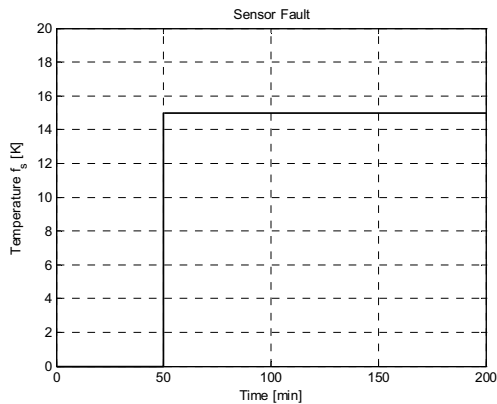


Figure 3: Sensor fault function

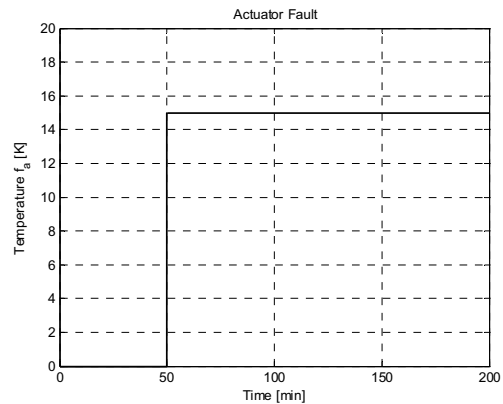


Figure 4: Actuator temperature fault function

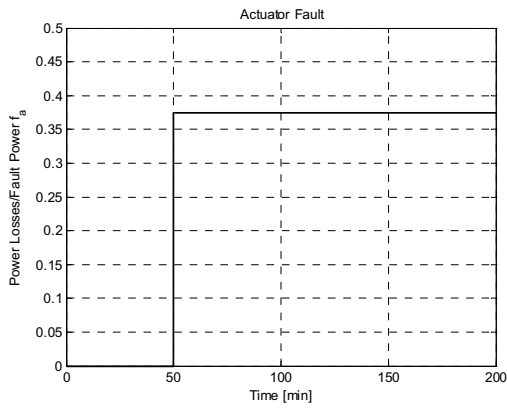


Figure 5: Actuator power losses fault function

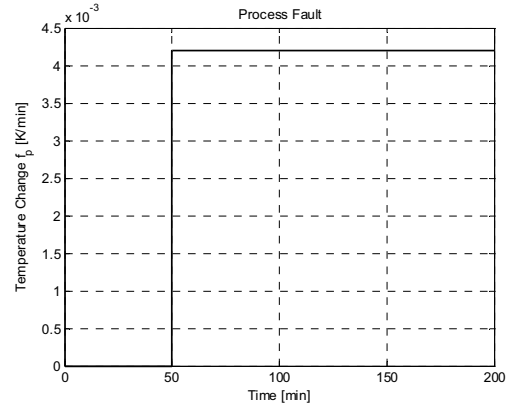


Figure 6: Process fault function

4.3 Simulation

The model and the observer are implemented in Matlab/Simulink. The simulation is structured so that the process model (including the faults) represents the wind turbine generator including the observer of the fault diagnosis system. The system is simulated for a total time of 200 min with a constant ambient temperature θ_{amb} and a sample time of $T = 100 \text{ ms}$. The power losses $P_i(k)$ are designed as a step function with the step at $t = 10 \text{ min}$. Each fault is simulated separately. For each simulation, three different observer gains \mathbf{L} are used ($L_1 < L_2 < L_3$). The gain \mathbf{L} defines how much the measured temperature $\theta(k)$ is influencing the model.

5. Results

In this section, the simulation results are presented divided by the fault described in section 4.2.

- $\theta_{non-faulty}(k)$ - the temperature with no fault in the system shows the expected heating as an logarithmic function starting at $t = 10 \text{ min}$ when the power losses $P_i(k)$ are unequal to zero.
- $\hat{\theta}_{L_1, L_2, L_3}(k)$ - the estimated temperatures shows how the model is adapting on the faulty system output depending on the used three different observer gains \mathbf{L} .

5.1 Sensor fault

First, the results of the sensor fault are shown in Figure 7. The following can be outlined:

- $\theta_{faulty}(k)$ - the temperature with a fault in the system shows the expected heating like the temperature with no fault until $t = 50 \text{ min}$. At this point, it can be seen that the simulated fault adds up with the temperature of the system for each time point.
- $\|\mathbf{r}(k)\|$ - the peak value shows a step with the height of the temperature fault at $t = 50 \text{ min}$ and later a decay to a constant peak difference between model and faulty system depending on the used three different observers gains \mathbf{L} .
- $\|\Delta\mathbf{r}(k)\|$ - the trend value shows a peak at $t = 50 \text{ min}$ because of the step in the $\theta_{faulty}(k)$ signal.

5.2 Actuator fault

Second, the results of the actuator fault are shown in Figure 8 and 9. The following can be outlined:

- $\theta_{faulty}(k)$ - the temperature with a fault in the system shows the expected heating like the temperature with no fault until $t = 50 \text{ min}$. At this point, it can be seen that the simulated fault adds up over time. Compared to the sensor fault it is not a step function.
- $\|\mathbf{r}(k)\|$ - the peak value shows a logarithmic behavior.
- $\|\Delta\mathbf{r}(k)\|$ - the trend value shows a peak at $t = 50 \text{ min}$ and a decay afterwards.

5.3 Processor fault

The processor fault shown in Figure 10 behaves in the same way as the actuator fault.

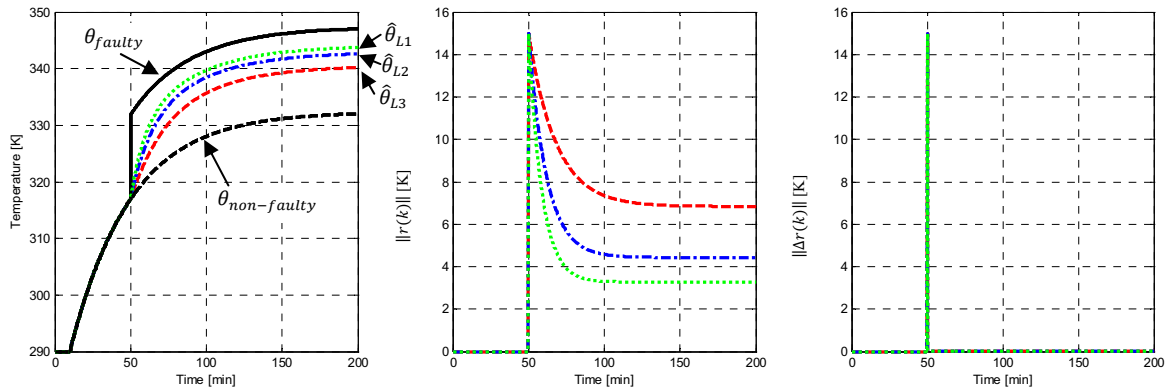


Figure 7: Simulation results for the sensor fault showing the temperatures (left), the peak value (middle) and the trend value (right) for the three different observer gains L .

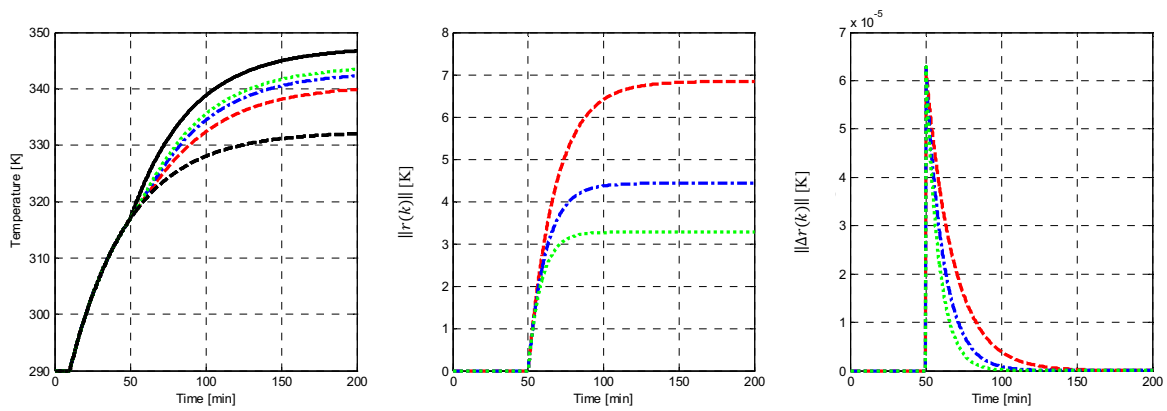


Figure 8: Simulation results for the actuator temperature fault showing the temperatures (left), the peak value (middle) and the trend value (right) for the three different observer gains L .

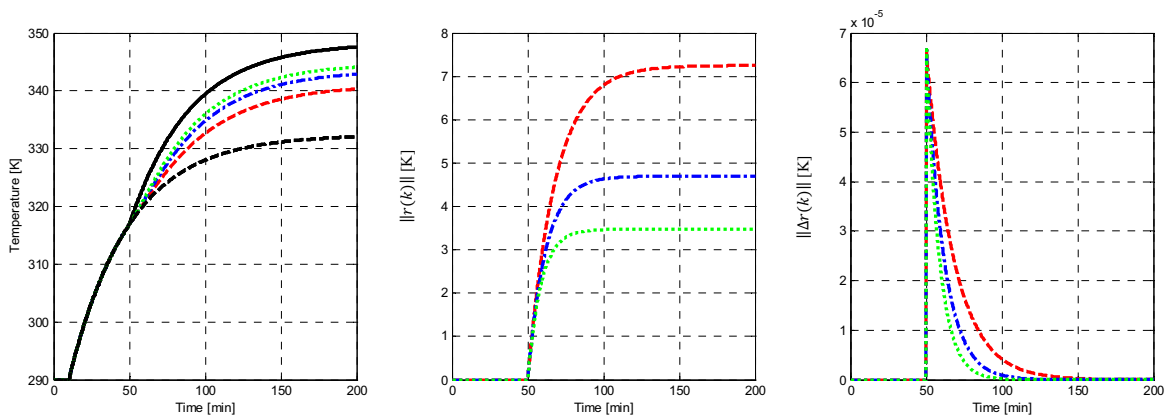


Figure 9: Simulation results for the actuator power losses fault showing the temperatures (left), the peak value (middle) and the trend value (right) for the three different observer gains L .

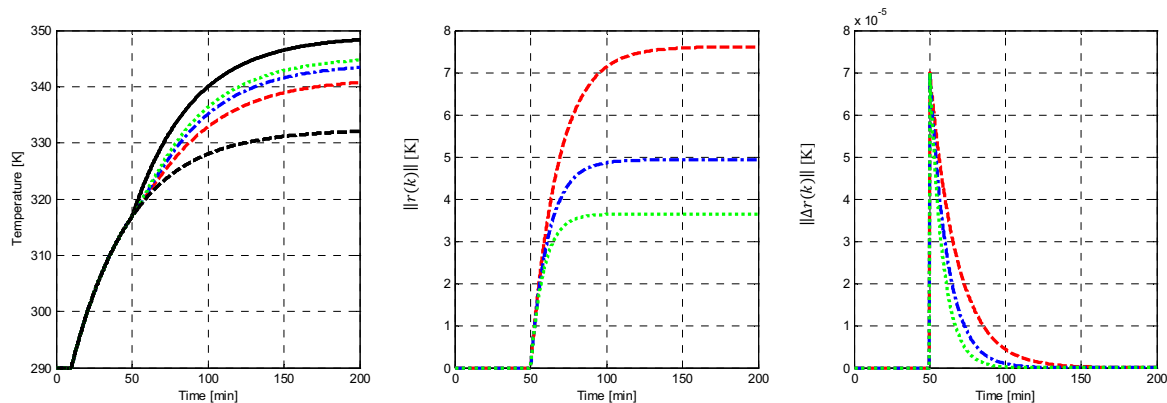


Figure 10: Simulation results for the process fault showing the temperatures (left), the peak value (middle) and the trend value (right) for the three different observer gains L .

6. Conclusion

Based on the results, we conclude the following points: First, for each simulated fault, a significant peak value J_{peak} can be calculated and plotted. The peak value shows two different behaviours depending where the fault occurs in the system. This presents a base for later fault isolation. It therefore can be distinguished if the fault occurs after (sensor fault) or inside/ before the feedback loop (actuator/ process fault). Second, the trend value J_{trend} only shows an evaluable behaviour if a sensor fault occurs. This also can be used to distinguish the different faults and help to identify a sensor fault. Third, the observer gain L plays a significant role in the detectability of the fault in the system. The L has to be chosen such that model uncertainties are compensated but fault detection is possible at the same time. It could be shown in the results that with varying L the behaviour of the peak and trend value is the same, except for variation in quantity. Therefore, by choosing a peak value threshold $J_{th,peak}$ and a trend value threshold $J_{th,trend}$, faults can be detected as presented in section 3.3. Furthermore the presented method is able to detect faults also in transient stages and is therefore a valuable tool to complement the widely used pre-set alert thresholds.

References

- Ding S. X., 2008, Model-based Fault Diagnosis Techniques, Springer-Verlag, Berlin Heidelberg, Germany
- Faulstich S., Hahn B., Tavner P. J., 2011, Wind turbine downtime and its importance for offshore deployment, Wind Energy, vol.14, no. 3, John Wiley & Sons, Ltd., doi: 10.1002/we.421
- Gertler J.J., 1988, Survey of model-based failure detection and isolation in complex plants, Control Systems Magazine, IEEE , vol.8, no.6, pp.3-11, doi: 10.1109/37.9163
- Gertler J.J., 1991, Analytical redundancy methods in fault detection and isolation, In Proceedings of IFAC/IAMCS symposium on safe process (Vol. 1, pp. 9-21)
- IEC Standard 60085 Electrical Insulation- Thermal Evaluation and Designation, 3rd ed., 2004 , page 11 table 1
- Isermann R., 1995, Model base fault detection and diagnosis methods, American Control Conference, Proceedings of the 1995 , vol.3, no., pp.1605-1609 vol.3, doi: 10.1109/ACC.1995.529778
- Nienhaus K., Hilbert M., 2012, Thermal analysis of a wind turbine generator by applying a model on real measurement data, Applied Measurements for Power Systems (AMPS), 2012 IEEE International Workshop on,doi: 10.1109/AMPS.2012.6344010
- Nienhaus K., Hilbert M., Baltés R., Berner C., 2012, Statistical and time domain signal analysis of the thermal behaviour of wind turbine drive train components under dynamic operation conditions, Journal of Physics Conference Series, vol.364, no.1, doi: 10.1088/1742-6596/364/1/012132